Journal of Hazardous Materials 187 (2011) 526–533

Contents lists available at ScienceDirect

Journal of Hazardous Materials

journal homepage: www.elsevier.com/locate/jhazmat

Ozonation of Cationic Red X-GRL in aqueous solution: Kinetics and modeling

Weirong Zhao[a,b,*], Feifei Liu[a], Yong Yang[a], Min Tan[a], Dongye Zhao[b]

[a] Department of Environmental Engineering, Zhejiang University, Hangzhou 310058, China
[b] Environmental Engineering Program, Department of Civil Engineering, Auburn University, Auburn, AL 36849, USA

ARTICLE INFO

Article history:
Received 6 October 2010
Received in revised form 14 January 2011
Accepted 14 January 2011
Available online 22 January 2011

Keywords:
Dyestuff
Ozone
Hydroxyl radical
Textile wastewater
Wastewater treatment

ABSTRACT

Ozonation of Cationic Red X-GRL was investigated in a semi-batch column reactor under various operating conditions such as gas flow rate Q_G, temperature T, initial concentration $C_{D,0}$, and pH. The relative contributions of ozone direct oxidation and •OH-facilitated indirect oxidation of the dyestuff were quantified, and the overall rate constant k_T and the kinetic regime of the reaction were determined by interpreting the experimental data with a newly derived kinetic model. The Hatta number of the reaction was found between 0.053 and 0.080, indicating that the reaction occurred in the liquid bulk, i.e. the slow kinetic regime. The ratio γ of indirect oxidation rate constant k_R to k_T decreased from 11.50% at pH 9.24 to 2.47% at pH 3.15. A mechanistically sounder model was derived to describe the reaction kinetics, which takes into account mechanisms of ozone decomposition and dyestuff degradation, and gas–liquid mass transfer. Good agreements were obtained between the experimental and calculated concentrations of Cationic Red X-GRL C_D, dissolved ozone C_A, ozone in off gas $C_{A,G}$, and nitrate. Furthermore, a model-based sensitivity analysis of $C_D/C_{D,0}$, C_A, and $C_{A,G}$ was performed with respect to various model parameters.

1. Introduction

Industrial dyeing processes lead to an estimated annual discharge of 30,000–150,000 tons of dyes into various receiving water bodies [1]. In addition to unpleasant aesthetic effects, dyestuffs have been associated with carcinogenic and/or teratogenic effects [1,2]. Yet, it has been a challenging technical issue to degrade dyestuffs from textile wastewater through conventional wastewater treatment processes because of their photo stability and resistance to biological degradation [1–4].

Ozonation has been very effective for degrading recalcitrant compounds in water and wastewater [5]. In the aqueous environment, ozone O_3 can decompose into hydroxyl radical •OH through a series of reactions including initiation and propagation [6–8]. Researchers have devoted extensive efforts for removing hazardous dyestuffs and examining the role of ozonation. Wang et al. [9] showed that ozonation is a highly effective way to remove the color of an azo dye, Remazol Black 5, and ozonation can enhance the biodegradability of azo dyes. Koch et al. [10] found that ozonation can almost completely degrade hydrolyzed Reactive Yellow 84. The azo group and sulfonic group were oxidized to nitrate and sulfate, respectively, and the main oxidation products of organic carbon are formic acid and oxalic acid [10]. Zhang et al. [11] identified the ozonation intermediates of hydrolyzed C.I. Reactive Red 120, and revealed the decomposition pathways during the ozonation process. Constapel et al. [12] studied ozonation of selected reactive dyes from textile wastewater, and revealed that the ozone treatment finally led to short-chained carboxylic acids and mineralized products. Shen et al. [13] asserted that ozonation appears to be a powerful tool for rapidly decolorizing wastewater containing textile dyes without forming appreciable waste residues.

On the other hand, ozonation involves complex gas–liquid processes where mass transfer and chemical reactions can control the overall kinetics [14,15]. Wu and Wang [16] developed a model to predict the enhancement factor of ozone mass transfer in ozonation of azo dye in a semi-batch column reactor. Based on relative contributions of direct ozonation and •OH-facilitated indirect oxidation to the overall dye degradation, Lopez-Lopez et al. [17] proposed a steady state model to determine the mass transfer, self-decomposition, and solubility parameters of ozone. Recently, Tokumura et al. [18] examined the ozone decolorization and mineralization of azo dye Orange II based on a model consisting of the ozone direct oxidation rate and gas–liquid mass transfer. However, there has been little information available on modeling the overall ozonation kinetics considering the overall mechanisms such as gas–liquid mass transfer, and chemical reactions with both ozone and •OH. Furthermore, a sound mathematical model is highly desirable to aid in the understanding of the ozonation process and to facilitate sound design and application of the process. Such a model could facilitate interpretation and prediction of temporal

* Corresponding author at: Department of Environmental Engineering, Zhejiang University, Hangzhou 310058, China. Tel.: +86 571 8898 2032; fax: +86 571 8898 2032.
E-mail address: weirong@mail.hz.zj.cn (W. Zhao).

0304-3894/$ – see front matter © 2011 Elsevier B.V. All rights reserved.
doi:10.1016/j.jhazmat.2011.01.071

performance of ozonation with respects to ozone direct reaction and •OH indirect reaction of dyes, and such model-based analyses can reveal the intrinsic relationships among the chemical reaction rate, mass transfer parameters of gas–liquid interface, concentration of intermediates and products, and reaction conditions [19]. Lastly, the model should be extensible so that modifications in reaction mechanism or rates can be incorporated into the modeling framework [14,15].

Applying tertiary butanol (TBA) as a scavenger to inhibit the reaction between •OH and Cationic Red X-GRL, our previous studies [20] determined the direct ozone reaction rate (i.e. in the absence of •OH-mediated indirect oxidation). In the present work, oxidation of the azo dye Cationic Red X-GRL by ozone direct reaction coupled with •OH indirect reaction was investigated in the semi-batch column reactor under various operating conditions such as gas flow rate Q_G, temperature T, initial Cationic Red X-GRL concentration $C_{D,0}$, and pH. The overall rate constants and the kinetic regime of the reaction between the oxidants and the dyestuff were determined by interpreting the experimental data with the new kinetic model. A mechanically sounder kinetic model was derived based on mechanisms of ozone decomposition and dyestuff degradation, and taking into account gas–liquid mass transfer. Furthermore, a sensitivity analysis was performed using the model aim to gain deeper insight into the degradation kinetics and mechanisms.

2. Materials and methods

Most of the information related to this section can be found in previous papers [20,21]. The commercial azo dye Cationic Red X-GRL was purified by the methanol recrystallization method. The molecular weight of the Cationic Red X-GRL is 356.84 g mol^{-1}, and its maximum absorbance wavelength is at 530 nm.

Ozonation tests were carried out in a 3.5 L semi-batch Pyrex glass column reactor submerged in a thermostatic bath to keep the temperature at the desired value ±0.5 °C as described in a previous work [20]. The reactor was equipped with inlets for gas (ozone–oxygen) feeding, water sampling, off gas, and temperature measurement. The Cationic Red X-GRL solutions buffered with orthophosphoric salt which was prepared by adding sodium hydroxide to adjust pH of orthophosphoric acid solution to desired pH values and the ionic strength I was set to 0.1 M. The ozone–oxygen mixture was produced in a CHYF-3A ozone generator (Rongxing Elec., China) to which oxygen was fed from a commercial cylinder. The input and off gas mass concentrations of ozone were determined iodometrically [20]. Then, the ozone partial pressure P_A in the gas phase was determined by the relationship of input and off gas mass concentration of ozone. Samples taken from reactor periodically were analysed for Cationic Red X-GRL using a UV–vis spectrophotometer (Pgeneral, China), where samples were scanned at a wavelength ranging from 800 to 200 nm. The concentration of ozone in aqueous solution C_A was also measured colorimetrically by the Indigo method [20] at 600 nm which does not interfere with the absorbance of Cationic Red X-GRL.

The values of the volumetric mass transfer coefficient k_La were obtained from a previous study [20] and are listed in Table 1. Previous direct oxidation experiments [20] determined that the stoichiometric ratio z of ozone to Cationic Red X-GRL is 4.

The Henry's law constants of ozone in water as a function of pH and T were obtained from Sotelo et al. [22]. By means of Henry's law, the equilibrium concentration of ozone C_A^* was deduced and are listed in Table 1. The diffusivity of ozone D_A in water was obtained from Matrozov et al. [23] as 1.08, 1.24, 1.42, 1.61, and 1.80×10^{-9} m^2 s^{-1} at 288, 293, 298, 303, and 308 K, respectively.

Table 1
Influence of experimental conditions on conversion of Cationic Red X-GRL, and the calculated model parameters.

Run	T(K)	pH	Q_G (L h^{-1})	P_A (kPa)	$C_A^* \times 10^{-4}$ (M)	$C_{D,0} \times 10^4$ (M)	$1 - C_D/C_{D,0}$					$-dC_D/dt \times 10^7$ (M s^{-1})		$k_La \times 10^3$ (s^{-1})	E	k_D (M^{-1} s^{-1})	k_T (M^{-1} s^{-1})	$\alpha_R \times 10^2$	$\gamma \times 10^{10}$	$Ha \times 10^3$
							1 min	2 min	3 min	4 min	5 min	6 min								
1	298	3.15	100	1.78	1.42	1.34	0.172	0.370	0.542	0.715	0.814	0.877	4.88	12.25	1.12	203	208	2.47	3.02	54
2	298	5.75	100	1.72	1.28	1.38	0.186	0.365	0.545	0.676	0.793	0.877	4.95	12.25	1.11	206	212	2.92	3.65	55
3	298	8.14	100	1.74	1.21	1.30	0.193	0.390	0.562	0.679	0.785	0.871	5.46	12.25	1.47	203	217	6.25	7.97	54
4	298	9.24	100	1.80	1.21	1.44	0.198	0.411	0.562	0.730	0.821	0.887	6.04	12.25	1.62	202	228	11.50	15.44	59
5	298	3.15	100	1.79	1.43	2.12	0.133	0.296	0.455	0.578	0.674	0.768	5.71	12.25	1.30	203	211	3.74	4.64	68
6	298	5.75	100	1.76	1.31	2.02	0.160	0.329	0.464	0.593	0.696	0.770	5.80	12.25	1.45	209	213	1.51	1.88	67
7	298	8.14	100	1.73	1.21	2.05	0.186	0.390	0.550	0.696	0.799	0.867	6.97	12.25	1.89	198	207	3.95	4.81	66
8	298	9.24	100	1.72	1.16	2.18	0.193	0.413	0.564	0.677	0.766	0.834	7.34	12.25	2.07	209	230	9.28	12.56	72
9	298	8.14	70	1.82	1.27	1.33	0.289	0.522	0.700	0.805	0.874	0.929	5.65	6.95	2.56	199	206	3.40	4.12	65
10	298	8.14	40	1.76	1.23	1.36	0.136	0.248	0.370	0.485	0.568	0.660	3.12	4.80	2.12	205	208	1.39	1.71	80
11	288	5.75	100	1.68	1.60	1.38	0.132	0.374	0.598	0.725	0.838	0.906	4.72	8.64	1.36	161	164	1.83	1.77	63
12	293	5.75	100	1.74	1.46	1.38	0.232	0.340	0.527	0.706	0.804	0.897	4.92	10.55	1.28	192	196	2.03	2.33	59
13	303	5.75	100	1.80	1.19	1.41	0.204	0.427	0.611	0.716	0.812	0.889	5.09	13.59	1.26	225	228	1.15	1.54	53
14	308	5.75	100	1.78	1.06	1.47	0.232	0.470	0.645	0.774	0.863	0.931	5.79	13.85	1.58	252	255	1.29	1.94	57

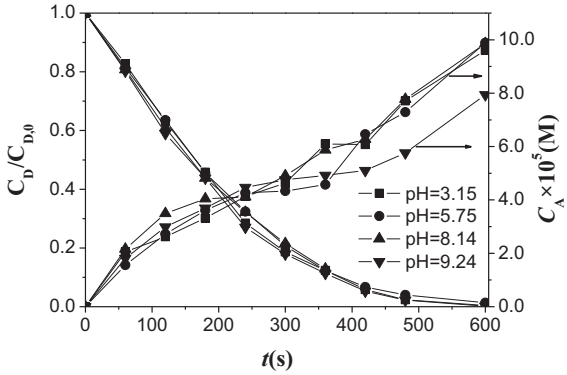

Fig. 1. Degradation of Cationic Red X-GRL $C_D/C_{D,0}$ and accumulation of dissolved ozone C_A at various pH's (Runs 1–4 in Table 1).

3. Results and discussion

3.1. Influence of reaction variables

Experiments of Cationic Red X-GRL degradation by ozone were carried out at various gas flow rate Q_G, temperature T, initial Cationic Red X-GRL concentration $C_{D,0}$, and pH. Table 1 shows the conversion $1 - C_D/C_{D,0}$ and degradation rate of Cationic Red X-GRL $-dC_D/dt$ at various times under various operating conditions.

Results from Runs 1–4 (Table 1) indicate that the effect of pH is modest: the degradation rate increases from $4.88 \times 10^{-7}\,M^{-1}\,s^{-1}$ at pH 3.15 to $6.04 \times 10^{-7}\,M^{-1}\,s^{-1}$ at pH 9.24. Increasing pH can increase the hydroxyl radical concentration, and then the indirect oxidation rate of Cationic Red X-GRL. On the other hand, however, the equilibrium concentration of ozone C_A^* is decreased at elevated pH, thereby lowering the direct oxidation rate of ozone.

It is evident from Fig. 1 that the dissolved ozone C_A accumulates with reaction time. Because the reaction is in the slow kinetic regime, which is confirmed later on (Section 3.2), the C_A is accumulated.

The gas flow rate Q_G affects volumetric mass transfer coefficient, and thus, increasing Q_G enhances the Cationic Red X-GRL degradation, as shown in Table 1. For example, increasing Q_G from 40 (Run 10) to 100 L h^{-1} (Run 3) increases the conversion of Cationic Red X-GRL from 66.0 to 87.1% at 300 s and degradation rate from 3.12 to $5.46 \times 10^{-7}\,M\,s^{-1}$.

Temperature can pose some opposing effects on the overall reaction rate. For example, when T is increased, the direct oxidation rate is increased [20], while C_A^* is decreased. The former effect is stronger than the later. As a result, the overall conversion and degradation rate of Cationic Red X-GRL increases with increasing T as shown in Table 1 (Runs 2, 11–14).

The influence of initial Cationic Red X-GRL concentration $C_{D,0}$ on the degradation rate of Cationic Red X-GRL can be revealed by comparing Runs 1–5, 2–6, 3–7, and 4–8 in Table 1: the degradation rate increases with increasing $C_{D,0}$.

3.2. Determination of gas–liquid mass transfer regime and kinetic parameters

According to the film theory, when absorption of a gas into a solution is accompanied by an irreversible chemical reaction with a compound dissolved in the liquid, the gas absorption rate $N_A a$ in the bulk liquid phase (slow kinetic regime) is given by [20,24]:

$$N_A a = k_L a C_A^* E = -\frac{z dC_D}{dt} + \frac{dC_A}{dt} \quad (1)$$

where E is the enhancement factor defined as the ratio of the rate of absorption in the presence of a chemical reaction to the maximum rate of pure physical absorption, z is the stoichiometric ratio for the ozone–Cationic Red X-GRL reaction.

As the term dC_A/dt is always <9% of term $-zdC_D/dt$ in all experimental results, the term dC_A/dt can be neglected to simplify the mathematical manipulation. Thus, the enhancement factor E can be calculated via [20]:

$$E = -\frac{z dC_D}{k_L a C_A^* dt} \quad (2)$$

Table 1 shows the E values obtained at $t = 0$. In all cases, the E values are <3, indicating that the reaction develops in the bulk liquid, i.e. in the slow kinetic regime [20,24].

Assuming that the direct oxidation rate k_D of Cationic Red X-GRL follows the first order rate law with respect to both ozone and Cationic Red X-GRL, and indirect oxidation rate k_R of Cationic Red X-GRL is also first order with respect to both •OH and Cationic Red X-GRL [19,20,25]. Then, the overall degradation rate can be described as:

$$-\frac{dC_D}{dt} = k_D C_D C_A + k_R C_D C_{\bullet OH} \quad (3)$$

In Eq. (3), the k_D was determined in our previous study [20] using 50 mM tertiary butanol as a scavenger to inhibit the reaction between •OH and Cationic Red X-GRL. Indirect oxidation rate k_R was determined to be $1.7 \times 10^{10}\,M^{-1}\,s^{-1}$ employing a competitive oxidation method by using phenol as a reference agent. Further information can be found in Text S1 of the Supplementary Information.

According to von Gunten [26] and Eq. (24) that will be shown later, the concentration of •OH is proportional to the concentration of dissolved ozone,

$$\gamma = \frac{C_{\bullet OH}}{C_A} \quad (4)$$

where the γ represents the fraction of decomposition of zone into •OH in certain pH.

Then, Eq. (3) can be transformed to:

$$-\frac{dC_D}{dt} = k_D C_D C_A + k_R \gamma C_D C_A = (k_D + k_R \gamma) C_D C_A = k_T C_D C_A \quad (5)$$

where k_T is the overall oxidation rate constant.

Eq. (5) can be integrated with initial condition: $t = 0$, $C_D = C_{D,0}$, yielding,

$$-\ln\left(\frac{C_D}{C_{D,0}}\right) = k_T \int_0^t C_A dt \quad (6)$$

Then, k_T can be calculated by fitting Eq. (6) to the experimental reaction rate data given in Table 1. For example, Fig. 2 shows the

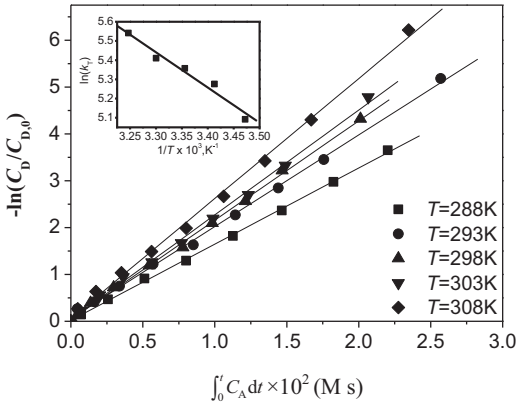

Fig. 2. Determination of the overall reaction rate constant k_T at various temperatures (Runs 2 and 11–14 in Table 1).

calculation of k_T at various temperatures. As shown in Fig. 2, the proposed rate law offered a reasonably good fit to the data in all cases.

In order to quantify the contribution of •OH-facilitated indirect oxidation, a proportionality constant α_R represents the degradation fraction of Cationic Red X-GRL by indirect oxidation rate over the overall reaction rate is introduced, defined as:

$$\alpha_R = \frac{k_R\gamma}{k_D + k_R\gamma} = \frac{k_R\gamma}{k_T} = 1 - \frac{k_D}{k_T} \quad (7)$$

According to Eq. (7), γ can be acquired through:

$$\gamma = \alpha_R \frac{k_T}{k_R} \quad (8)$$

Table 1 gives the calculated α_R and γ values. At pH 9.24, α_R is ca. 10% and γ lies between 10^{-9} and 10^{-10} [26,27]; and the values of α_R and γ decreased with decreasing pH. Therefore, the •OH-facilitated indirect oxidation is rather weak in this work.

Data in Table 1 also indicate that the k_T is clearly pH-dependent. When pH was raised from 3.15 (Run 1) to 9.24 (Run 4), k_T increases from 208 to 228 M^{-1} s^{-1} and α_R increases from 2.47 to 11.50 × 10^{-2}. Because the concentration of •OH is influenced by the concentration of hydroxyl ion, α_R increases with pH. Table 1 also indicates that k_T is influenced by temperature strongly. As temperature was increased from 288 (Run 11) to 308 K (Run14), k_T increases from 164 to 255 M^{-1} s^{-1}. Thus, the overall rate constant can be expressed by a modified Arrhenius equation as follows [20]:

$$k_T = k_0' \exp\left(-\frac{E_{a,obs}}{RT}\right)(OH^-)^m \quad (9)$$

where $E_{a,obs}$ is the observed activation energy, m is the exponential constant of concentration of OH^-, and is the pre-exponential factor of modified Arrhenius equation.

According to Eq. (9), $E_{a,obs}$ can be calculated by non-linear regression analysis of k_T as a function of T and pH. The following correlation equation was obtained based on the results in Runs 1–14 of Table 1,

$$k_T = 108,013 \exp\left(\frac{-15,298}{RT}\right)(OH^-)^{0.0037}\ (M^{-1}s^{-1}), \quad r = 0.981 \quad (10)$$

with $E_{a,obs}$ = 15.298 kJ mol^{-1} and m = 0.0037.

The $E_{a,obs}$ is slightly lower than an activation energy of 15.538 kJ mol^{-1} for direct ozone oxidation of the dyestuff in a previous work [20].

The k_T values shown in Table 1 were used to verify the condition of slow kinetic regime. For this purpose, the dimensionless Hatta number Ha was determined for all experiments. For a second order irreversible reaction, the Ha takes the form [24]:

$$Ha = \left(\frac{D_A k_T C_D}{k_L^2}\right)^{1/2} \quad (11)$$

This Ha allows for ascertaining the type of kinetic regime: a low value of Ha between 0.02 and 0.3 indicates that the reaction occurs in the slow regime, whereas a value higher than 3 points to the fast regime; and a value between 0.3 and 3 correspond to the moderately fast regime [24]. Table 1 shows the calculated Ha values at the initial reaction time. The values ranged between 0.053 and 0.080 in all cases, indicating that the all reactions occurred in the slow regime. Therefore, the reaction between ozone and Cationic Red X-GRL occurs in the liquid bulk.

3.3. General mechanism of ozonation of Cationic Red X-GRL

Table 2 summarizes the reaction steps in the ozonation system. Ozone can decompose into •OH through a series of chain reactions, including an initiation step (reaction 1) followed by a series of propagation steps (reactions (2)–(7)) [6–8]. Ozone and •OH in the aqueous solution are able to break aromatic rings [25,28–30]. Reaction between radicals (reactions (8)–(10)) can terminate the propagation of radicals. It is worth mentioning that the phosphorous species such as H_3PO_4, $H_2PO_4^-$, and HPO_4^{2-} can act as weak scavengers of •OH (reactions (11)–(13)) because the •OH reaction rate constant of these species at range of 10^5–10^7 M^{-1} s^{-1} are much

Table 2
Reaction mechanisms in the ozonation: reaction steps and rate constants.

No.	Reaction	Rate constant	Ref.
1	$O_3 + OH^- \xrightarrow{k_1} HO_2^\bullet + O_2^{\bullet-}$	$k_1 = 7.0 \times 10^1\ M^{-1}\ s^{-1}$	[33]
2	$HO_2^\bullet \overset{K_a}{\rightleftarrows} O_2^{\bullet-} + H^+$	$K_a = 10^{-4.8}$	[33]
3	$O_3 + O_2^{\bullet-} \xrightarrow{k_2} O_3^{\bullet-} + O_2$	$k_2 = 1.6 \times 10^9\ M^{-1}\ s^{-1}$	[33]
4	$O_3^{\bullet-} + H^+ \underset{k_{-3}}{\overset{k_3}{\rightleftarrows}} HO_3^\bullet$	$k_3 = 5.2 \times 10^{10}\ M^{-1}\ s^{-1} k^{-3} = 3.3 \times 10^2\ s^{-1}$	[33]
5	$HO_3^\bullet \xrightarrow{k_4} {}^\bullet OH + O_2$	$k_4 = 1.4 \times 10^5\ s^{-1}$	[33]
6	${}^\bullet OH + O_3 \xrightarrow{k_5} HO_4^\bullet$	$k_5 = 3.0 \times 10^9\ M^{-1}\ s^{-1}$	[33]
7	$HO_4^\bullet \xrightarrow{k_6} HO_2^\bullet + O_2$	$k_6 = 2.8 \times 10^4\ s^{-1}$	[33]
8	$HO_4^\bullet + HO_4^\bullet \xrightarrow{k_7} H_2O_2 + 2O_3$	$k_7 = 5.0 \times 10^9\ M^{-1}\ s^{-1}$	[33]
9	$HO_4^\bullet + HO_3^\bullet \xrightarrow{k_8} H_2O_2 + O_3 + O_2$	$k_8 = 5.0 \times 10^9\ M^{-1}\ s^{-1}$	[33]
10	$HO_4^\bullet + HO_2^\bullet \xrightarrow{k_9} H_2O + O_3 + O_2$	$k_9 = 10^{10}\ M^{-1}\ s^{-1}$	[33]
11	$H_3PO_4 + {}^\bullet OH \xrightarrow{k_{PH,1}} H_2O + H_2PO_4^\bullet$	$k_{PH,1} = 2.6 \times 10^6\ M^{-1}\ s^{-1}$	[32]
12	$H_2PO_4^- + {}^\bullet OH \xrightarrow{k_{PH,2}} OH^- + H_2PO_4^\bullet$	$k_{PH,2} = 2.2 \times 10^7\ M^{-1}\ s^{-1}$	[32]
13	$HPO_4^{2-} + {}^\bullet OH \xrightarrow{k_{PH,3}} OH^- + HPO_4^{-\bullet}$	$k_{PH,3} = 7.9 \times 10^5\ M^{-1}\ s^{-1}$	[32]
14	$H_3PO_4 \overset{K_1}{\rightleftarrows} H^+ + H_2PO_4^-$	$K_1 = 10^{-2.2}$	[32]
15	$H_2PO_4^- \overset{K_2}{\rightleftarrows} H^+ + HPO_4^{2-}$	$K_2 = 10^{-7.2}$	[32]
16	$HPO_4^{2-} \overset{K_3}{\rightleftarrows} H^+ + PO_4^{3-}$	$K_3 = 10^{-12.3}$	[32]
17	$TBA + {}^\bullet OH \xrightarrow{k_{TBA}}$ final product	$k_{TBA} = 5 \times 10^8\ M^{-1}\ s^{-1}$	[34]
18	$D + zO_3 \xrightarrow{k_D} P$	$k_D = 108{,}810 \exp(-15{,}538/RT)\ M^{-1}\ s^{-1}$	[20]
19	$D + {}^\bullet OH \xrightarrow{k_R} P$	$k_R = 1.7 \times 10^{10}\ M^{-1}\ s^{-1}$	
20	$P_i + {}^\bullet OH \xrightarrow{k_{P_i}}$ final or more intermediate		

slower than common rate constant range of 10^8–10^{10} M^{-1} s^{-1} [6–8,19,27,31].

As can be seen in Section 3.6, the maximum concentration of •OH is ca. 10^{-13} M at pH 10, the second order reaction rate between radicals (reactions (8)–(10)) is much slower than reactions between compounds, and radical and compounds. Therefore, the reaction rates between radicals (reactions (8)–(10)) can be ignored in the kinetic research later.

The intermediate products can influence the ozonation kinetics (reactions (18) and (19) in Table 2). This is because the intermediates also consume ozone and •OH [32]. Our previous work [21] revealed that 1 mol Cationic Red X-GRL consumes 4 mol ozone in direct ozonation reaction. This ozone demand can be explained by a simplified degradation mechanism [20].

As •OH can be consumed by TBA with a relatively high rate (reaction (17) in Table 2), TBA can inhibit the indirect oxidation of other compounds by •OH. By the way, the TBA is a weak surfactant that can influence the k_La of ozone in mass transfer.

Based on the reaction mechanisms and mass transfer parameters of semi-batch column reactor, the following rate models are formulated through mole balance equations for the compounds such as Cationic Red X-GRL, dissolved ozone, ozone in off gas, and nitrate. Assuming complete water and gas mixing, and considering that the reaction of ozone with Cationic Red X-GRL takes place in the slow kinetic regime the kinetic models for the semi-batch column reactor are deduced as follows:

For ozone in water,

$$\frac{dC_A}{dt} = k_La(C_A^* - C_A) - \sum r_i = k_La\left(\frac{(P_A + P_{A,in})/2}{H} - C_A\right) - \sum r_i \quad (12)$$

where P_A and $P_{A,in}$ are the ozone partial pressure in the off gas and input gas, respectively, H is the Henry's constant, and $\sum r_i$ is the decomposition term of ozone due to chemical reactions defined as follows:

$$\sum r_i = (4k_DC_D + k_1C_{OH^-} + k_2C_{O_2^{\bullet -}} + k_5C_{\bullet OH})C_A \quad (13)$$

For ozone in the gas phase,

$$\frac{dC_{A,G}}{dt} = \frac{Q_G}{V_G}\left(\frac{P_{A,in}}{RT} - C_{A,G}\right) - k_La\frac{V}{V_G}\left(\frac{(P_A + P_{A,in})/2}{H} - C_A\right) \quad (14)$$

where V_G and V are the cumulative volume of gas in the reactor (0.060 L), and the volume of the liquid phase (3.5 L), respectively.

For Cationic Red X-GRL, the degradation rate can be acquired by Eq. (3).

For nitrate,

$$\frac{dC_{NO_3^-}}{dt} = k_DC_DC_A \quad (15)$$

3.4. Determination of radical concentrations

Based on the mechanism of Table 2 and Eqs. (3), (12)–(15), the formation rates of radicals in the system can be described by Eqs. (16)–(20):

$$\frac{dC_{HO_2\bullet}}{dt} + \frac{dC_{O_2^{\bullet -}}}{dt} = 2k_1C_{OH^-}C_A - k_2C_{O_2^{\bullet -}}C_A + k_6C_{HO_4\bullet} \quad (16)$$

$$\begin{aligned}\frac{dC_{\bullet OH}}{dt} &= k_4C_{HO_3\bullet} - k_5C_{\bullet OH}C_A - k_RC_{\bullet OH}C_D - k_{TBA}C_{\bullet OH}C_{TBA} \\ &\quad -(k_{PH,1}C_{PH,1} + k_{PH,2}C_{PH,2} + k_{PH,3}C_{PH,3})C_{\bullet OH} \\ &\quad - \sum k_{P_i}C_{\bullet OH}C_{P_i} \\ &= k_4C_{HO_3\bullet} - k_5C_{\bullet OH}C_A - k_RC_{\bullet OH}C_D - k_{TBA}C_{\bullet OH}C_{TBA} \\ &\quad - \sum k_{PH,i}C_{\bullet OH}C_{PH,i} - \sum k_{P_i}C_{\bullet OH}C_{P_i}\end{aligned} \quad (17)$$

$$\frac{dC_{HO_3\bullet}}{dt} = k_3C_{H^+}C_{O_3^{\bullet -}} - (k_{-3} + k_4)C_{HO_3\bullet} \quad (18)$$

$$\frac{dC_{O_3^{\bullet -}}}{dt} = k_2C_{O_2^{\bullet -}}C_A - k_3C_{H^+}C_{O_3^{\bullet -}} + k_{-3}C_{HO_3\bullet} \quad (19)$$

$$\frac{dC_{HO_4\bullet}}{dt} = k_5C_{\bullet OH}C_A - k_6C_{HO_4\bullet} \quad (20)$$

Assuming that the system is at pseudo-steady state, the hydroxyl and superoxide ion radical concentrations can be obtained by the following equations:

$$C_{\bullet OH} = \frac{2k_1C_{OH^-}C_A}{k_RC_D + k_{TBA}C_{TBA} + \sum k_{PH,i}C_{PH,i} + \sum k_{P_i}C_{P_i}} \quad (21)$$

$$C_{O_2^{\bullet -}} = \frac{2k_1C_{OH^-} + k_5C_{\bullet OH}}{k_2} \quad (22)$$

Due to the unknown compositions of the ozonated Cationic Red X-GRL solution, the indirect reaction term of Cationic Red X-GRL and •OH in the denominator of Eq. (22) and intermediates (reactions (19) and (20) in Table 2) are assumed constant and can be expressed as follows:

$$k_RC_D + \sum k_{P_i}C_{P_i} = k_RC_{D,0} \quad (23)$$

The rate constants, k_R and k_{P_i} of •OH-mediated reactions are of similar magnitude because the unselective character of •OH. According to a previous study [21], the reduction of TOC (total organic carbon) in a similar system is <5.7% in 600 s, indicating that mineralization of Cationic Red X-GRL is weak. In addition, the organic intermediates are similar in oxidation nature to their parent compound Cationic Red X-GRL. The effective collision between total organic carbon and •OH, and consumption of •OH would keep rather stable during the ozonation process. Therefore, Eq. (23) appears reasonable under these experiments.Thus,

$$C_{\bullet OH} = \frac{2k_1C_{OH^-}C_A}{k_RC_{D,0} + k_{TBA}C_{TBA} + \sum k_{PH,i}C_{PH,i}} \quad (24)$$

It was calculated that the value of $k_RC_{D,0}$ is 100 times greater than $\sum k_{PH,i}C_{PH,i}$ in the experimental conditions. The scavenger effect of reactions (11)–(13) in Table 2 is trivial. Thus, it can be deducted from Eq. (24) that the concentration of •OH is proportional to the concentration of ozone without TBA.

Substituting Eqs. (23) and (24) into Eq. (13) gives:

$$\sum r_i = \left(4k_DC_D + 3k_1C_{OH^-} + \frac{4k_5k_1C_{OH^-}}{k_RC_{D,0} + k_{TBA}C_{TBA} + \sum k_{PH,i}C_{PH,i}}\right)C_A \quad (25)$$

As can be seen from Eq. (25), the decomposition term of ozone $\sum r_i$ is proportional to the C_D with $z = 4$, and to the concentration of hydroxyl ion in solution.

3.5. Prediction of concentrations of Cationic Red X-GRL, dissolved ozone, ozone in off gas, and nitrate

The first order differential Eqs. (3), (12)–(15) were solved numerically to obtain the concentration profiles of Cationic Red X-GRL, dissolved ozone, ozone in off gas, and nitrate. In this work, the fourth order Runge–Kutta method was used for solving the equation set with the following initial conditions:

$$t = 0, \quad C_D = C_{D,0}, \quad C_A = 0, \quad C_{A,G} = 0, \quad \text{and } C_{nitrate} = 0 \quad (26)$$

For examples, Fig. 3 shows the transient concentration profiles of measured and calculated C_D, C_A, $C_{A,G}$, and $C_{nitrate}$, respectively. Fig. 3a shows the results at pH 8.14 in Run 3 of Table 1. The model is able to adequately predict the experimentally measured C_D as the reactor reached the well-mixed state rapidly.

Fig. 3b shows that the experimentally measured C_A and calculated C_A matched fairly well. The maximum deviation appears at the end of reaction, which can be attributed to that fact that the model calculation did not account for the additional ozone consumption

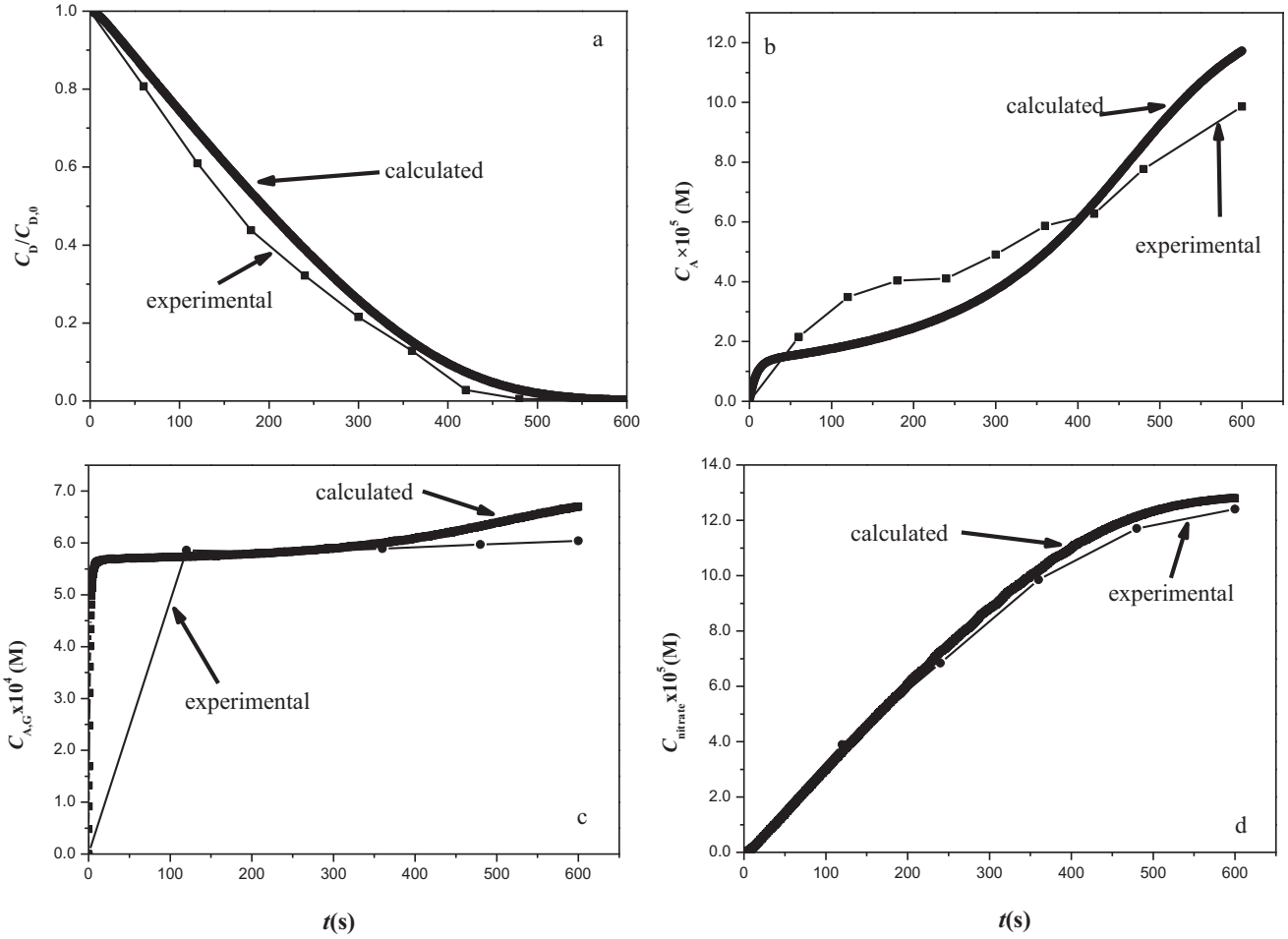

Fig. 3. Calculated and experimental concentrations of (a) Cationic Red X-GRL, (b) dissolved ozone, (c) off gas ozone, and (d) nitrate (Run 3 in Table 1).

for degradation of intermediates. For the $C_{A,G}$ (see Fig. 3c), the same trend as C_A was observed between the experimental and calculated concentrations. Finally, Fig. 3d shows that the model predicts the nitrate production rate very well.

3.6. Sensitivity analysis of experimental parameters

Sensitivity analysis of the model was performed with first order differential Eqs. (3), (12)–(15) and with respect to the parameters (pH, T, P_A, Q_G, and C_{TBA}). The following conditions were assumed where applicable: $Q_G = 100\,L\,h^{-1}$, $C_{D,0} = 1.3 \times 10^{-4}$ M, $T = 298$ K, and $P_A = 1.75$ kPa, with the initial conditions as Eq. (26).

The pH of water is probably the most complex parameter affecting the ozonation processes. Fig. 4a–c shows the calculated results of C_D, C_A, and $C_{A,G}$ at pH 3, 7, and 10, respectively. The degradation of Cationic Red X-GRL and $C_{A,G}$ are influenced slightly (Fig. 4a and c), while C_A decreases markedly as pH is varied from 3 to 10. The greater pH sensitivity of C_A is due to the fact that reaction (1) in Table 2 takes place faster at a higher pH where more •OH are produced (Fig. 4b). Eqs. (27) and (28) define the characteristics of •OH-mediated indirect reaction ratio by calculating $\alpha_{R,cal}$ and direct ozonation ratio by calculating $\alpha_{D,cal}$. The concentration of •OH is increased from 10^{-20} M at pH 3 to 10^{-16} M at pH 7 and 10^{-13} M at pH 10, and the $\alpha_{R,cal}$ is increased from 10^{-8} at pH 3 to 10^{-4} at pH 7 and 0.34 at pH 10.

$$\alpha_{R,cal} = \frac{k_R C_D C_{\bullet OH}}{k_D C_D C_A + k_R C_D C_{\bullet OH}} = \frac{k_R C_{\bullet OH}}{k_D C_A + k_R C_{\bullet OH}} \quad (27)$$

$$\alpha_{D,cal} = \frac{k_D C_D C_A}{k_D C_D C_A + k_R C_D C_{\bullet OH}} = \frac{k_D C_A}{k_D C_A + k_R C_{\bullet OH}} = 1 - \alpha_{R,cal} \quad (28)$$

Fig. 4d–f shows the calculated results of C_D, C_A, and $C_{A,G}$ at T of 288, 298, and 308 K, respectively. With increasing T, the C_A^* deceases [22], whereas $k_L a$ and k_T increase. As a result, the degradation of Cationic Red X-GRL is increased modestly with increasing temperature (Fig. 4d), while C_A and $C_{A,G}$ are decreased notably (Fig. 4e and f).

Fig. 4g–i shows the calculated results of C_D, C_A, and $C_{A,G}$ at P_A of 1, 1.75, and 2.5 kPa, respectively. With increasing P_A, the mass transfer driving force, i.e. the ozone concentration gradient across the gaseous phase and liquid phase is increased. Therefore, the degradation of Cationic Red X-GRL, C_A, and $C_{A,G}$ are increased.

Fig. 4j–l shows the calculated results of C_D, C_A, and $C_{A,G}$ at Q_G of 40, 70, and 100 L h^{-1}, respectively. With increasing Q_G, mass transfer coefficient is increased. Therefore, the degradation of Cationic Red X-GRL, C_A, and $C_{A,G}$ are increased.

Fig. 4m–o shows the calculated results of C_D, C_A, and $C_{A,G}$ at 0 and 50 mM of C_{TBA}, respectively. The degradation of Cationic Red X-GRL (Fig. 4m), C_A, and $C_{A,G}$ (Fig. 4n and o) decrease with increasing C_{TBA}. At pH 10, the concentration of •OH decreases from 10^{-13} M without TBA to 10^{-14} M with a TBA of 50×10^{-3} M, and the $\alpha_{R,cal}$ decreases from 0.34 without TBA to 0.041 with 50×10^{-3} M of TBA. Evidently, TBA can exert strong scavenging effect on the ozonation processes.

Therefore, the parameters such as pH and C_{TBA} can influence $C_D/C_{D,0}$, C_A, and $C_{A,G}$ apparently through the influencing of formation of •OH, while the T influence $C_D/C_{D,0}$, and $C_{A,G}$ moderately

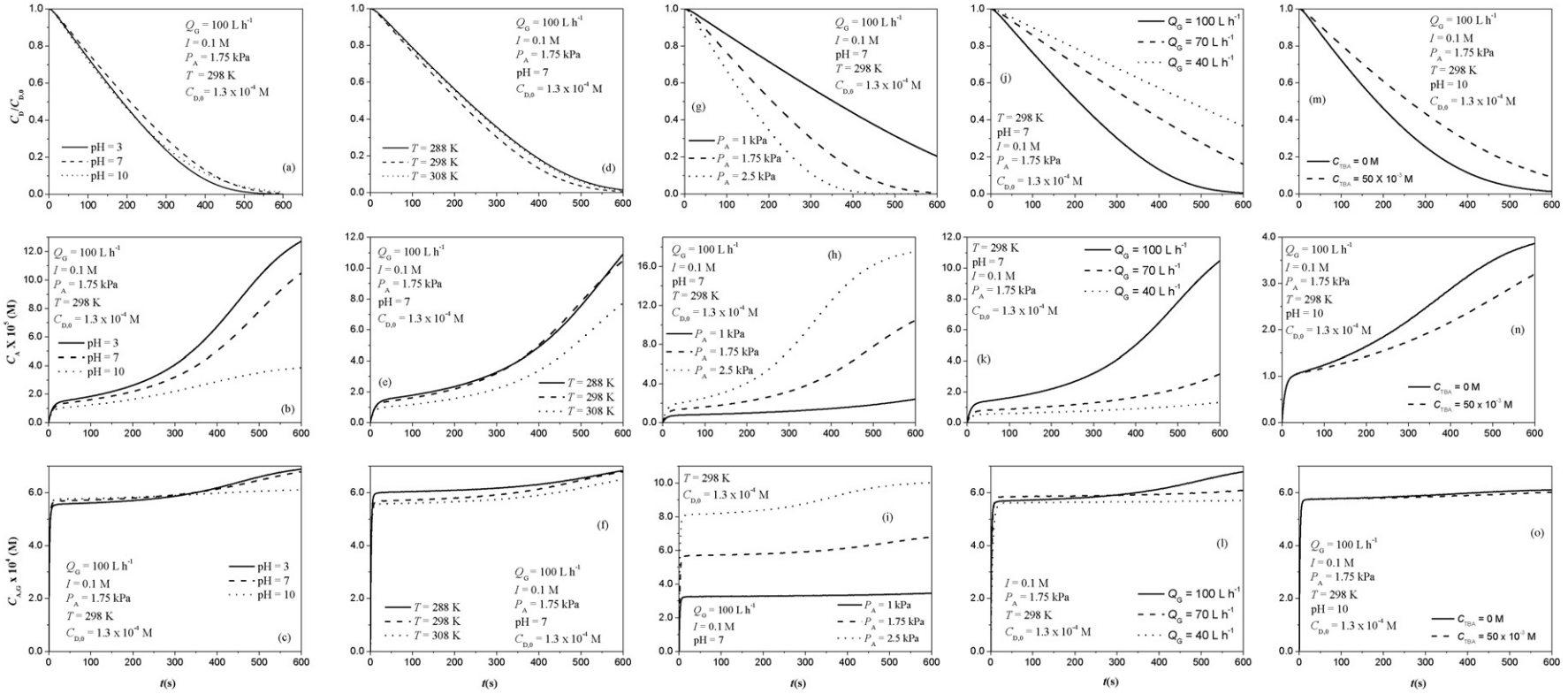

Fig. 4. Sensitivity analyses of C_D, C_A, and $C_{A,G}$ with respect to (a–c) pH, (d–f) T, (g–i) P_A, (j–l) Q_G, and (m–o) C_{TBA}.

through the influencing of C_A. The parameters such as P_A and Q_G can influence $C_D/C_{D,0}$, C_A, and $C_{A,G}$ strongly through the influencing of mass transfer parameters of the semi-batch bubble column reactor.

4. Conclusions

The results from this work indicate that coupled absorption of ozone into aqueous solution and subsequent ozonation of Cationic Red X-GRL can be described by an irreversible second order reaction kinetic model. The reaction occurs in the bulk liquid, corresponding to the slow kinetic regime. While Cationic Red X-GRL had been thought degradable via both direct ozonation and indirect •OH-mediated oxidation, model calculations indicate that the degradation is predominantly facilitated by direct ozonation. Even at pH 9.24, the •OH-mediated indirect oxidation is rather weak with a α_R of ~10% and γ between 10^{-9} and 10^{-10}. Based on our experimental data, a correlation equation was obtained through a modified Arrhenius equation, which correlates the overall rate constant with T and pH in the ozonation system. The correlation gave an observed activation energy $E_{a,obs}$ of 15.298 kJ mol^{-1} and an exponential constant m of 0.0037.

Kinetic modeling of pollutant ozonation in water is a suitable tool for predicting process efficiency and reactor design. For ozonation of Cationic Red X-GRL, a mechanistically sounder kinetic model was derived by considering mass transfer, ozone decomposition mechanisms, and Cationic Red X-GRL degradation pathways. The parameters such as pH and C_{TBA} can influence $C_D/C_{D,0}$, C_A, and $C_{A,G}$ apparently through the influencing of formation of •OH, while T influences $C_D/C_{D,0}$ and $C_{A,G}$ moderately through influencing C_A. The parameters such as P_A and Q_G can influence $C_D/C_{D,0}$, C_A, and $C_{A,G}$ strongly through influencing mass transfer parameters of the semi-batch bubble column reactor. Overall, the model is able to adequately interpret the experimental concentrations of Cationic Red X-GRL, dissolved ozone, off gas ozone, and nitrate.

Acknowledgement

This research was partially supported by The National Water Pollution Control and Management Project of China (2008ZX07101–006).

Appendix A. Supplementary data

Supplementary data associated with this article can be found, in the online version, at doi:10.1016/j.jhazmat.2011.01.071.

References

[1] A.M. Talarposhti, T. Donnelly, G.K. Anderson, Colour removal from a simulated dye wastewater using a two-phase anaerobic packed bed reactor, Water Res. 35 (2001) 425–432.
[2] S.M.D.G.U. de Souza, K.A.S. Bonilla, A.A.U. de Souza, Removal of COD and color from hydrolyzed textile azo dye by combined ozonation and biological treatment, J. Hazard. Mater. 179 (2010) 35–42.
[3] S. Wijetunga, X.F. Li, C. Jian, Effect of organic load on decolourization of textile wastewater containing acid dyes in upflow anaerobic sludge blanket reactor, J. Hazard. Mater. 177 (2010) 792–798.
[4] H. Wang, X.W. Zheng, J.Q. Su, Y. Tian, X.J. Xiong, T.L. Zheng, Biological decolorization of the reactive dyes Reactive Black 5 by a novel isolated bacterial strain Enterobacter sp. EC3, J. Hazard. Mater. 171 (2009) 654–659.
[5] M.M. Huber, A. Gobel, A. Joss, N. Hermann, D. Loffler, C.S. Mcardell, A. Ried, H. Siegrist, T.A. Ternes, U. von Gunten, Oxidation of pharmaceuticals during ozonation of municipal wastewater effluents: a pilot study, Environ. Sci. Technol. 39 (2005) 4290–4299.
[6] J. Staehelin, R.E. Buhler, J. Hoigne, Ozone decomposition in water studied by pulse-radiolysis. 2. OH and HO_4 as chain intermediates, J. Phys. Chem. 88 (1984) 5999–6004.
[7] R.E. Buhler, J. Staehelin, J. Hoigne, Ozone decomposition in water studied by pulse-radiolysis. 1. HO_2/O_2^- and HO_3/O_3^- as intermediates, J. Phys. Chem. 88 (1984) 2560–2564.
[8] J. Staehelin, J. Hoigne, Decomposition of ozone in water in the presence of organic solutes acting as promoters and inhibitors of radical chain reactions, Environ. Sci. Technol. 19 (1985) 1206–1213.
[9] C. Wang, A. Yediler, D. Lienert, Z. Wang, A. Kettrup, Ozonation of an azo dye C.I. Remazol Black 5 and toxicological assessment of its oxidation products, Chemosphere 52 (2003) 1225–1232.
[10] M. Koch, A. Yediler, D. Lienert, G. Insel, A. Kettrup, Ozonation of hydrolyzed azo dye reactive yellow 84 (CI), Chemosphere 46 (2002) 109–113.
[11] F.F. Zhang, A. Yediler, X.M. Liang, Decomposition pathways and reaction intermediate formation of the purified, hydrolyzed azo reactive dye C.I. Reactive Red 120 during ozonation, Chemosphere 67 (2007) 712–717.
[12] M. Constapel, M. Schellentrager, J.M. Marzinkowski, S. Gab, Degradation of reactive dyes in wastewater from the textile industry by ozone: analysis of the products by accurate masses, Water Res. 43 (2009) 733–743.
[13] J.M. Shen, Z.L. Chen, Z.Z. Xu, X.Y. Li, B.B. Xu, F. Qi, Kinetics and mechanism of degradation of p-chloronitrobenzene in water by ozonation, J. Hazard. Mater. 152 (2008) 1325–1331.
[14] P. Chelme-Ayala, M.G. El-Din, D.W. Smith, Kinetics and mechanism of the degradation of two pesticides in aqueous solutions by ozonation, Chemosphere 78 (2010) 557–562.
[15] J.A. Pedit, K.J. Iwamasa, C.T. Miller, W.H. Glaze, Development and application of a gas–liquid contactor model for simulating advanced oxidation processes, Environ. Sci. Technol. 31 (1997) 2791–2796.
[16] J.N. Wu, T.W. Wang, Ozonation of aqueous azo dye in a semi-batch reactor, Water Res. 35 (2001) 1093–1099.
[17] A. Lopez-Lopez, J.S. Pic, H. Debellefontaine, Ozonation of azo dye in a semi-batch reactor: a determination of the molecular and radical contributions, Chemosphere 66 (2007) 2120–2126.
[18] M. Tokumura, T. Katoh, H. Ohata, Y. Kawase, Dynamic modeling and simulation of ozonation in a semibatch bubble column reactor: decolorization and mineralization of azo dye orange II by ozone, Ind. Eng. Chem. Res. 48 (2009) 7965–7975.
[19] F.J. Benitez, F.J. Real, J.L. Acero, C. Garcia, Kinetics of the transformation of phenyl-urea herbicides during ozonation of natural waters: rate constants and model predictions, Water Res. 41 (2007) 4073–4084.
[20] W.R. Zhao, Z.B. Wu, D.H. Wang, Ozone direct oxidation kinetics of Cationic Red X-GRL in aqueous solution, J. Hazard. Mater. 137 (2006) 1859–1865.
[21] W.R. Zhao, H.X. Shi, D.H. Wang, Ozonation of Cationic Red X-GRL in aqueous solution: degradation and mechanism, Chemosphere 57 (2004) 1189–1199.
[22] J.L. Sotelo, F.J. Beltran, F.J. Benitez, J. Beltranheredia, Ozone decomposition in water – kinetic-study, Ind. Eng. Chem. Res. 26 (1987) 39–43.
[23] V.I. Matrozov, S.A. Kashtanov, A.M. Stepanov, B.A. Tregubov, Experimental-determination of coefficient of molecular-diffusion of ozone in water, J. Appl. Chem. USSR 49 (1976) 1111–1114.
[24] F.J. Beltrán, Ozone Reaction Kinetics for Water and Wastewater Systems, Lewis Publishers, Boca Raton, Fla, 2004.
[25] B. Ning, N.J.D. Graham, Y.P. Zhang, Degradation of octylphenol and nonylphenol by ozone. Part II. Indirect reaction, Chemosphere 68 (2007) 1173–1179.
[26] U. von Gunten, Ozonation of drinking water. Part I. Oxidation kinetics and product formation, Water Res. 37 (2003) 1443–1467.
[27] N.K.V. Leitner, B. Roshani, Kinetic of benzotriazole oxidation by ozone and hydroxyl radical, Water Res. 44 (2010) 2058–2066.
[28] W.R. Chen, C.M. Sharpless, K.G. Linden, I.H.M. Suffet, Treatment of volatile organic chemicals on the EPA contaminant candidate list using ozonation and the O_3^-/H_2O_2 advanced oxidation process, Environ. Sci. Technol. 40 (2006) 2734–2739.
[29] K.S. Tay, N.A. Rahman, M.R. Abas, Degradation of DEET by ozonation in aqueous solution, Chemosphere 76 (2009) 1296–1302.
[30] B. Ning, N.J.D. Graham, Y.P. Zhang, Degradation of octylphenol and nonylphenol by ozone. Part I. Direct reaction, Chemosphere 68 (2007) 1163–1172.
[31] F.J. Beltran, M. Gonzalez, F.J. Rivas, P. Alvarez, Aqueous UV radiation and UV/H_2O_2 oxidation of atrazine first degradation products: deethylatrazine and deisopropylatrazine, Environ. Toxicol. Chem. 15 (1996) 868–872.
[32] F.J. Beltran, J. Rivas, P.M. Alvarez, M.A. Alonso, B. Acedo, A kinetic model for advanced oxidation processes of aromatic hydrocarbons in water: application to phenanthrene and nitrobenzene, Ind. Eng. Chem. Res. 38 (1999) 4189–4199.
[33] J. Staehelin, J. Hoigne, Decomposition of ozone in water – rate of initiation by hydroxide ions and hydrogen-peroxide, Environ. Sci. Technol. 16 (1982) 676–681.
[34] J. Hoigne, H. Bader, Rate constants of reactions of ozone with organic and inorganic-compounds in water. 1. Non-dissociating organic-compounds, Water Res. 17 (1983) 173–183.